Water Resources Research

RESEARCH ARTICLE
10.1029/2019WR027012

Analytical Solution of Suspended Sediment Concentration Profile: Relevance of Dispersive Flow Term in Vegetated Channels

Wenxin Huai[1], **Liu Yang**[1], **and Yakun Guo**[2]

[1]State Key Laboratory of Water Resources and Hydropower Engineering Science, Wuhan University, Wuhan, China, [2]Faculty of Engineering and Informatics, University of Bradford, Bradford, UK

Key Points:

- A dispersive model is proposed to investigate the sediment transport in the vegetated open channels with parameters fitted with experiments
- Analytical solution of the vertical suspended sediment concentration profile is derived for submerged and emergent vegetated open channels
- The effects of dispersion on suspended sediment concentration in the vegetated channels is demonstrated by the double-averaging method

Correspondence to:
W. Huai,
wxhuai@whu.edu.cn

Citation:
Huai, W., Yang, L., & Guo, Y. (2020). Analytical solution of suspended sediment concentration profile: Relevance of dispersive flow term invegetated channels. *Water Resources Research*, *56*, e2019WR027012. https://doi.org/10.1029/2019WR027012

Received 26 DEC 2019
Accepted 18 JUN 2020
Accepted article online 22 JUN 2020

Abstract Simulation of suspended sediment concentration (SSC) has great significance in predicting the sediment transport rate, vegetation growth, and the river ecosystem in channels. The present study focuses on investigating the vertical SSC profile in the vegetated open channel flows. To this end, a model of the dispersive flux is proposed in which the dispersive coefficient is expressed as partitioned linear profile above or below the half height of vegetation. The double-averaging method, that is, time-spatial average, is applied to investigate the vertical SSC profile in the vegetated open channel flows. The analytical solution of SSC in both submerged and emergent vegetated open channel flows is obtained by solving the vertical double-averaging sediment advection-diffusion equation. The morphological coefficient, a key factor of dispersive coefficient, is obtained by fitting the existing experimental data. The analytically predicted SSC agrees well with the experimental measurements, indicating that the proposed model can be used to accurately predict the SSC in the vegetated open channel flows. Results show that the dispersive term can be ignored in the region without vegetation, while the dispersive term has significant effect on the vertical SSC profile within the region of vegetation. The present study demonstrates that the dispersive coefficient is closely related to vegetation density, vegetation structure, and stem Reynolds number but has little relation with flow depth. With a few exceptions, the absolute value of the dispersive coefficient decreases with the increase of vegetation density and increases with the increase of stem Reynolds number in the submerged vegetated open channels.

1. Introduction

Aquatic vegetation in the vegetated open channel flows can significantly affect flow velocity and turbulence structure and momentum exchange processes (Huai, Zeng, et al., 2009; Li et al., 2015, 2019; Nepf, 2012) as well as the sediment transport (Le Bouteiller & Venditti, 2015; S. Li & Katul, 2019; Yang & Nepf, 2019). Previous studies (Li et al., 2018; Wang et al., 2016) showed that the vertical profile of suspended sediment concentration (referred as SSC hereafter), an important characteristic for waterway ecosystem, is much more complicated in the vegetated open channels than that in channels without vegetation, due to the great variation of the turbulent strength in the vertical direction. Studies of Kim et al. (2018) and Västilä and Järvelä (2018) on the suspended sediment deposition within and around a circular vegetation patch showed that the vegetation enhanced the deposition of sediment in the vegetation region. These studies showed that aquatic vegetation greatly affects the sediment transport rate. The previously dominant methodologies of simulating the suspended sediment transport are based on the time-averaging Navier-Stokes equations or advection-diffusion equations, including turbulent diffusion model (Kundu, 2019; Li et al., 2018), two-phase flow model (Fu et al., 2005), and flume experimental model (Kim et al., 2018; Västilä & Järvelä, 2018). In the vegetated open channels, the spatial heterogeneity of flow field is significantly enhanced by the presence of aquatic vegetation. In order to improve the simulation accuracy in the vegetated open channel flows, the double-averaging methodology is introduced to extend the time-averaging flow field to time-spatial averaging field (Nikora, McEwan, et al., 2007; Wang et al., 2014).

The double-averaging method is usually applied to the large eddy simulation (LES), direct numerical simulation (DNS), and physical model to study the spatial heterogeneity in the open channel flow and airflow. To investigate the impact of heterogeneity on edge-flow dynamics, Boudreault et al. (2017) applied double-averaging method to the LES to simulate the forest-edge flows. Their results showed that the

forest heterogeneity facilitated flow penetration into the vegetation (i.e., trees and plants). In the roughness region, for example, rough bed, the heterogeneity is strong. Han et al. (2017) and Stoesser and Nikora (2008) applied the LES with the double-averaging method to evaluate the effect of the roughness on the rough-bed flows. In addition, Coceal et al. (2006, 2007, 2008) used the regular arrays of cubical obstacles as the rough bed to study the turbulent flow and the dispersive stress in roughness flows with the DNS and the double-averaging method. Laboratory experiment is another methodology to study the flow with spatial heterogeneity. Moltchanov et al. (2015) and Poggi and Katul (2008a) carried out flume experiments to investigate the effect of the spatial heterogeneity on the flow structure in the vegetated open channel flows, while Spiller et al. (2015) conducted flume experiments to examine the role of the heterogeneity in nonuniform steady and unsteady flow over a rough bed. These numerical and experimental studies showed that the double-averaging method can reduce the inconvenience of time-averaging variables in volume resulted from the spatial heterogeneity. In addition, the dispersive flux (or stress), an additional key term in the double-averaging method, is generated due to the deviation of time-averaging field from space averaging field (Tanino & Nepf, 2008a).

So far, the dispersive term in the vegetated open channels has been poorly defined, making it difficult to clearly express the dispersive stress. Florens et al. (2013) conducted laboratory experiments and measured the fluctuation velocity using particle image velocimetry (PIV) to investigate the dispersive stress in the vegetated open channel flows. Poggi, Katual, and Albertson (2004), Poggi, Porporato, and Ridolfi (2004), and Poggi and Katul (2008b) conducted flume experiments with the submerged vegetation made of rigid cylindrical rods. They found that the maximum value of the dispersive stress had comparable magnitude (almost 30% of the total stress) with the Reynolds stress (almost 70% of the total stress) within the vegetation region for sparse-vegetated flow and was trivial for dense-vegetated flow. They also found that the dispersive stress appeared to decrease with the increase of vegetation density. Righetti (2008) conducted experiment with the natural vegetation (*Salix pentandra*) and showed that the dispersive stress was large and could not be ignored in natural flexible vegetated flow. These experimental studies revealed that (i) the dispersive stress was significant within the vegetation region and insignificant in the region without vegetation and (ii) the value of the dispersive stress reached the maximum value at the position close to the half height of vegetation and gradually decreased toward both the channel bottom and the water surface. In addition, the dispersive stress is significant not only in the vegetated flow but also in the rough-bed flow (Nikora, McLean, et al., 2007). The study of Nikora, McLean, et al. (2007) for the flow over a rough bed showed that the double-averaging method could identify the specific flow layers and flow types and the dispersive stress existed in the roughness region of the rough-bed flow.

Most previous studies only focused on the phenomenon of the dispersive stress. To the authors' best knowledge, so far, little knowledge exists about the effect of the dispersive flux on the vertical SSC profile, the application of the dispersive term on the mass transport, and the model of the dispersive coefficient. This motivates this study, which focuses on developing a new dispersive coefficient model and investigating the relationship of dispersive strength with canopy density and the vertical SSC profile in the steady vegetated open channel flows. Recently, Tsai and Huang (2019) simulated the suspended sediment transport with the stochastic Lagrangian model. However, their simulated vertical SSC profile was inconsistent with the experimental observations (see Figure 11 in the literature of Tsai & Huang, 2019). Huai et al. (2019) took dispersion into account and applied the random displacement model, also a Lagrangian model, to simulate the vertical SSC profile in the vegetated open channel flows. Though their simulated results were almost consistent with the experimental observations, some deviation still existed in the region of vegetation for the submerged vegetated open channel flow. The reason for this deviation in the vegetation region may be due to the hypothesis that the profile of the dispersive coefficient was the same as the turbulent diffusion coefficient with different magnitude. This could mean that the distribution of the dispersive coefficient is different from the turbulent diffusion coefficient in the vegetated open channel flows. Yuuki and Okabe (2002) used the dispersive coefficient, the averaged longitudinal flow velocity of cross section, and the averaged SSC of cross section to model the dispersive flux. As discussed above, the comparable magnitude of dispersion only exists in the vegetation region, and the local SSC differs from the averaged SSC of cross section. Therefore, from the point of view of the physical mechanism, it will be much better to use the local SSC to scale the dispersive flux. In order to improve the simulation of the vertical SSC profile, in this study, the double-averaging method is thus applied to investigate the sediment transport in the

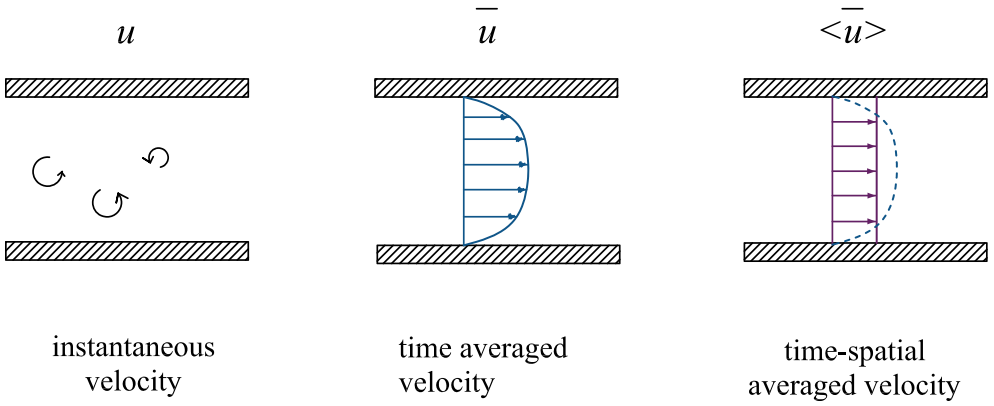

Figure 1. The schematic diagram of time-spatial averaging method for platforms flow.

vegetated open channel flows by assuming that the dispersive term only exists in the vegetation region. In order to reduce the deviation caused by the application of the averaged SSC of cross section, a new approximation approach is then proposed in this study to express the dispersive flux of suspended sediment, where the dispersive flux is proportional to the local SSC in the vegetated open channel flows. The analytical solution of the vertical SSC profile is obtained by solving the double-averaging advection-diffusion equations, which are influenced by vegetation density, vegetation structure, flow characteristics, and the spatial arrangement of vegetation.

2. Theory

2.1. Double-Averaging Method

Though the double-averaging method can be found in previous studies (e.g., Nikora, McEwan, et al., 2007; Nikora, McLean, et al., 2007), we present a brief description for convenience and completeness. To this end, the flow between the platforms, as shown in Figure 1, is taken as an example to demonstrate the concept of the double-averaging method. The instantaneous longitudinal flow velocity (denoted as u) can be decomposed as $u = \overline{u} + u'$ based on the Reynold's decomposition approach, while the time-averaging velocity can be further decomposed as $\overline{u} = \langle \overline{u} \rangle + u''$. In these decompositions, the overbar denotes the time-averaged variables, the single prime represents the fluctuation velocity, that is, the deviation of instantaneous variables from the time-averaging variables; the double prime denotes the time-averaged deviations from spatial-averaged variables and the symbol $\langle\rangle$ represents the spatially averaged variables. Instantaneous velocity, therefore, can be expressed as $u = \langle \overline{u} \rangle + u'' + u'$ in the time-spatial averaging flow field. This means that the double-averaging method includes two main steps: (1) first, applying time averaging to the equations for instantaneous variables and (2) second, applying the spatial averaging to the equations which have already been averaged in the time domain.

Though the double-averaging method has been widely applied to investigate the flow field in rough open channel and river flow, the method has been hardly ever applied to estimate the vertical SSC profile in the vegetated open channel flows. In this paper, the authors will propose a new model for describing the dispersion in sediment-laden flow with vegetation and apply the double-averaging method to calculate the vertical SSC profile. The instantaneous advection-diffusion equation of sediment is written as following based on the mass conservation:

$$\frac{\partial c}{\partial t} + \frac{\partial (u_j c)}{\partial x_j} - \frac{\partial}{\partial x_j}\left(K_m \frac{\partial c}{\partial x_j}\right) + S = 0, \tag{1}$$

where t represents time, c is the instantaneous SSC, x_j is the jth direction ($x_1 = x$ represents the longitudinal direction; $x_2 = y$ represents the transverse direction; $x_3 = z$ represents the vertical direction), u_j (j = 1, 2, and 3) is the instantaneous flow velocity component in the directions of x, y, and z, respectively, K_m represents the molecular diffusion coefficient, and S represents the source or sink of sediment. The

first term in Equation 1 is the variation of SSC with time, the second term represents the transport of sediment advection flux in the x_j direction, and the third term is the transport of sediment molecular diffusion flux.

Applying the double-averaging approach by inserting the decomposed instantaneous variables of c, u_j, and S as $\varphi = \overline{\varphi} + \varphi'$ (where φ represents the variables) into Equation 1 yields

$$\frac{\partial}{\partial t}(\overline{c}+c')+\frac{\partial}{\partial x_j}\left[\left(\overline{u}_j+u_j'\right)\left(\overline{c}+c'\right)\right]-\frac{\partial}{\partial x_j}\left(K_m\frac{\partial(\overline{c}+c')}{\partial x_j}\right)+\overline{S}+S'=0. \tag{2}$$

Applying time averaging to Equation 2 yields

$$\frac{\partial}{\partial t}(\overline{\overline{c}+c'})+\frac{\partial}{\partial x_j}\left[\overline{\left(\overline{u}_j+u_j'\right)\left(\overline{c}+c'\right)}\right]-\frac{\partial}{\partial x_j}\left(\overline{K_m\frac{\partial(\overline{c}+c')}{\partial x_j}}\right)+\overline{S}+\overline{S'}=0. \tag{3}$$

According to the rules, $\overline{f+\varphi}=\overline{f}+\overline{\varphi}, \overline{\sigma f}=\sigma\overline{f}$, and $\overline{f'}=0$ (where f represents a variable and σ is a constant), Equation 3 can be simplified as (Tanino & Nepf, 2008a; Termini, 2019):

$$\frac{\partial\overline{c}}{\partial t}+\frac{\partial}{\partial x_j}\left(\overline{u}_j\overline{c}+\overline{u_j'c'}\right)-\frac{\partial}{\partial x_j}\left(K_m\frac{\partial\overline{c}}{\partial x_j}\right)+\overline{S}=0. \tag{4}$$

Using the decomposition of $\overline{c}, \overline{u}_j$, and $\overline{S}$ as $\overline{\varphi}=\langle\overline{\varphi}\rangle+\varphi''$, applying the spatial-averaging method and according to the rules, $\langle\varphi''\rangle=0$ and $\langle\langle\overline{\varphi}\rangle\rangle=\langle\overline{\varphi}\rangle$, Equation 4 can be expressed as

$$\frac{\partial\langle\overline{c}\rangle}{\partial t}+\frac{\partial\left(\langle\overline{u}_j\rangle\langle\overline{c}\rangle\right)}{\partial x_j}+\frac{\partial}{\partial x_j}\left(\langle\overline{u_j'c'}\rangle+\langle u_j''\,c''\rangle\right)-\frac{\partial}{\partial x_j}\left(K_m\frac{\partial\langle\overline{c}\rangle}{\partial x_j}\right)+\langle\overline{S}\rangle=0. \tag{5}$$

Equation 5 is the double-averaging advection-diffusion equation. The first term of Equation 5 expresses the variation of the double-averaging SSC with time. The second term is the transport of advection flux resulted from the averaged flow velocity. The third term is the transport of diffusive flux related to the turbulent fluctuations u_j', and the fourth term is the transport of the dispersive flux associated with the spatial heterogeneity of time-averaging velocity field. The molecular diffusion term is ignored as it is much smaller than the turbulent diffusion and the dispersive flux. Assuming that no sediment is added into the river, therefore, the sediment source/sink term $\langle\overline{S}\rangle$ can be written as $-\partial(\omega\langle\overline{c}\rangle)/\partial x_3$ (i.e., the transport of sediment settling flux) in sandy flow, where ω is the settling velocity of sediment particles. Furthermore, in the steady uniform open channel flow, one has $\frac{\partial\langle\overline{c}\rangle}{\partial t}=0, \partial\left(\langle\overline{u}_j\rangle\langle\overline{c}\rangle\right)/\partial x_j=0$ for $j=1, 2$, and $3, \partial\left(\langle\overline{u_j'c'}\rangle\right)/\partial x_j=0$, and $\partial(\langle u''\,c''\rangle)/\partial x_j=0$ for $j=1$ and 2 (i.e., in both the longitudinal and the transverse directions). Equation 5 can then be simplified as

$$\frac{\partial}{\partial x_3}\left(\langle\overline{u_3'c'}\rangle+\langle u_3''c''\rangle\right)-\frac{\partial(\omega\langle\overline{c}\rangle)}{\partial x_3}=0. \tag{6}$$

The additional dispersive flux term needs to be appropriately determined in order to accurately simulate the vertical SSC profile in the steady equilibrium vegetated open channel sediment-laden flow.

2.2. The Dispersive Flux

The turbulent diffusion flux in Equation 6 is determined by the Fickian transport theory (Termini, 2019; van Rijn, 1984; Yang & Choi, 2010):

$$\langle\overline{u_3'c'}\rangle=-K_z\frac{\partial\langle\overline{c}\rangle}{\partial x_3}=-K_z\frac{\partial C}{\partial z}, \tag{7}$$

where K_z represents the vertical turbulent diffusion coefficient. In Equation 7, for simplification, $\langle\overline{c}\rangle$ is replaced by C to represent the time-spatial-averaged SSC.

In flow without vegetation, the dispersive flux is usually ignored as it is much smaller than the turbulent flux. However, in the vegetated open channel flow, the dispersive flux cannot be ignored as the spatial heterogeneity is significantly strengthened by the presence of vegetation. This indicates that the dispersive flux has great effect on the vertical SSC profile in the vegetated open channel flow. In this study, we assume that the dispersive flux can be expressed as follows:

$$\langle u_3'' c'' \rangle = -K_D U C, \tag{8}$$

where K_D is the dispersive coefficient and U is the longitudinal averaged velocity of cross section and is used to scale the magnitude of the vertical averaged velocity that is difficult to obtain. Substituting Equations 7 and 8 into Equation 6 yields

$$\frac{\partial}{\partial z}\left(-K_z\frac{\partial C}{\partial z} - K_D U C\right) - \frac{\partial(\omega C)}{\partial z} = 0. \tag{9}$$

The sediment advection-diffusion equation of fully developed steady flow can then be simplified as follows:

$$\omega C + K_z\frac{dC}{dz} + K_D U C = A, \tag{10}$$

where A is an integral constant. Equation 10 shows that the first term (the downward sediment settling flux) has to balance with the second and third terms (the upward diffusion and the dispersive fluxes). As no sediment is added into or jumps out of river at the water surface, the integral constant A is equal to 0. Equation 10 then becomes

$$\omega C + K_z\frac{dC}{dz} + K_D U C = 0. \tag{11}$$

The vertical SSC profile in the steady vegetated open channel flows can then be obtained by solving Equation 11.

In this study, the dispersive coefficient K_D that is related to the spatial heterogeneity in the vegetated open channel flow is defined as a function of the vertical coordinate z. In order to simplify the dispersive model, we assume that the dispersive coefficient is equal to the product of a scale factor K_f multiplying the morphological coefficient k_m:

$$K_D = K_f k_m, \tag{12}$$

where the morphological coefficient k_m is a parameter reflecting the impact of flow field and vegetation (including the vegetation density, structure, and arrangement) on dispersion; the scale factor $K_f = 0.001$ is used to eliminate the influence induced by the application of the longitudinal sediment flux UC rather than the vertical sediment flux $u_3 C$ as well as to express the magnitude of the dispersive coefficient. Simulation shows that it is appropriate for the conditions investigated in this proposed model. According to the variation rules of the dispersive coefficient, k_m is equal to 0 in the flow without vegetation, where the magnitude of the dispersion term is much smaller than the diffusion and advection terms.

The effect of dispersion is significant due to strong heterogeneity generated by the presence of vegetation. As discussed above, extensive experimental studies have been conducted to investigate the profile of the dispersive stress in the vegetated open channel flow. These studies (Poggi, Porporato, & Ridolfi, 2004; Righetti, 2008; Stoesser & Nikora, 2008) showed that the variation of the dispersive stress was complicated but followed the similar law. They (Poggi, Porporato, & Ridolfi, 2004; Righetti, 2008; Stoesser & Nikora, 2008) found that the dispersive stress increased from the 0 at the channel bottom and reached the maximum value at almost the half height of vegetation and then decreased and approached 0 at the top of vegetation. As such, the morphological coefficient can be parameterized as follows:

$$k_m = \begin{cases} 0 & z \geq h \quad (a) \\ -\frac{2\theta}{h}z + 2\theta & \frac{h}{2} \leq z < h \quad (b) \\ \frac{2\theta}{h}z & z < \frac{h}{2} \quad (c) \end{cases}, \tag{13}$$

where h is the height of vegetation and the parameter θ is the value of the morphological coefficient at the half height of vegetation, where coefficient k_m reaches the maximum value. Equations 12 and 13 show that the dispersive coefficient is known when the value of θ is determined. The maximum value of the morphological coefficient can be obtained by fitting the available experimental data of SSC for various vegetation conditions.

3. Method

In order to investigate the effect of the dispersive flux on the vertical SSC profile in the vegetated open channel flow, the turbulent diffusion flux and the sediment settling flux need to be determined. Nepf (2004) conducted experiments to investigate the characteristic of the turbulent diffusion using the rigid straight rods as vegetation. The results showed that the turbulent diffusion coefficient approximated to the linear profile within the region of vegetation in the submerged vegetated open channel flow. The turbulent diffusion coefficient reached the maximum value at the top of vegetation and decreased linearly toward the water surface. Several formulas were proposed to simulate the turbulent diffusion coefficient in channels with the submerged vegetation. However, the turbulent diffusion coefficient remains almost a constant in the emergent vegetated open channel flow (Nepf, 1999). The settling velocity of sediments is another important parameter and can be estimated using the formula proposed by Zhang and Xie (1989) (see also Tan et al., 2018), which is applicable for both the laminar and the turbulent flow

$$\omega = \sqrt{\left(13.95\frac{\nu}{d}\right)^2 + 1.09\frac{\gamma_s - \gamma_f}{\gamma_f}gd} - 13.95\frac{\nu}{d}, \tag{14}$$

where ν represents the kinematic viscosity of water, g is the acceleration of gravity, γ_s and γ_f represent the bulk density of sediment and water, respectively, d is the representative size of sediment particles, and the median size of sediments is used in this study.

The analytical solution of the vertical SSC profile can be obtained by solving Equation 11 with the turbulent diffusion coefficient, the sediment settling velocity, as well as the dispersive coefficient determined in different vegetated open channel flows. The following sections introduce the methods for channels with the emergent and the submerged vegetation, respectively.

3.1. Channels With the Emergent Vegetation

Previous studies showed that majority of the flow momentum is absorbed by the vegetation elements induced drag instead of the resistance generated by channel bed in the vegetated open channel flows (Tanino & Nepf, 2008b; Wilson, 2007). The vertical turbulent diffusion coefficient $K_z(z)$ is homogenized due to the presence of the emergent aquatic vegetation (Nepf, 1999, 2004) and can be expressed as the following in dense vegetation flow ($a_v h > 0.1$) with the emergent cylindrical stems of uniform diameter:

$$K_z = \alpha\sqrt[3]{C_D a_v D}UD, \tag{15}$$

where D is the diameter of vegetation stem, C_D is the drag coefficient of vegetation, a_v is the frontal area density of vegetation (expressed as $a_v = nD$, n is the number of vegetation per unit area of channel bed), and α is a proportional factor, which is taken as 0.2 for the vertical turbulent diffusion coefficient and as 0.8 for the lateral turbulent diffusion coefficient in the emergent vegetated open channel flow (Nepf, 2004). In addition, α should slightly increase for the condition of dense vegetation. The value of C_D significantly depends on the density of vegetation and flow Reynolds number (Sonnenwald et al., 2019). In present study, according to the balance of vegetation drag with the streamwise component of gravity, the drag coefficient is evaluated as $C_D = 2gs/(a_v U^2)$ (where s is the slope of channel bed) for experimental conditions of different vegetation densities (Huai, Chen, et al., 2009).

Table 1
Experimental Parameters of Lu (2008) and Ikeda Et Al. (1991) in the Emergent Vegetated Open Channel Flows

Sources	Run number	$h(H)$ (m)	D (m)	s (10^{-3})	U (m/s)	u_* (m/s)	d (mm)	a_v (m^{-1})	C_D/
	D12-1	0.12	0.006	13.6	0.3343	0.1265	0.217	2.4	0.99
	D12-2	0.12	0.006	13.6	0.2918	0.1265	0.217	3.0	1.04
	D12-3	0.12	0.006	13.6	0.1690	0.1265	0.217	6.0	1.56
	D15-1	0.15	0.006	13.6	0.3321	0.1414	0.217	2.4	1.01
Lu	D15-2	0.15	0.006	13.6	0.2932	0.1414	0.217	3.0	1.03
	D15-3	0.15	0.006	13.6	0.1700	0.1414	0.217	6.0	1.54
	D18-1	0.18	0.006	13.6	0.3436	0.1549	0.217	2.4	0.94
	D18-2	0.18	0.006	13.6	0.2947	0.1549	0.217	3.0	1.02
	D18-3	0.18	0.006	13.6	0.1692	0.1549	0.217	6.0	1.55
Ikeda	Run 9	0.05	0.005	6.67	0.2858	0.0572	0.145	1.0	1.60

As the dispersive coefficient is different in the regions of $z > h/2$ and $z < h/2$, the analytical solution of Equation 11 should be solved respectively at different layers with $z = h/2$ as the critical height. Integrating Equation 11 using the turbulent diffusion coefficient determined by Equation 15 and the dispersive coefficient determined by Equations 12 and 13 yields the profiles of the vertical SSC in the emergent vegetated open channel flow:

$$C = C_a \exp\left(\frac{\theta K_f U}{hK_z}\left(z^2 - {z_a}^2\right) - \frac{2\theta K_f U + \omega}{K_z}(z - z_a)\right) \text{ for } z \geq \frac{h}{2}, \tag{16a}$$

$$C = C_a \exp\left(-\frac{\theta K_f U}{hK_z}\left(z^2 - \frac{h^2}{4}\right) - \frac{\omega}{K_z}\left(z - \frac{h}{2}\right)\right) \text{ for } z < \frac{h}{2}, \tag{16b}$$

where z_a and C_a are the referenced height and the corresponding referenced SSC, respectively. In this study, z_a is taken as the half height of the flow depth, namely, $z_a = H/2$ (H is the flow depth) and $H = h$ in the emergent vegetated flow.

Experiments conducted by Ikeda et al. (1991) and Lu (2008) are used to fit the dispersive coefficient and to validate the analytical model. The experimental parameters are summarized in Table 1. In their experiments, SSC was measured in the emergent vegetated (rigid cylindrical rods) flow for various vegetation densities. To calculate the vertical SSC profile, the turbulent diffusion coefficient K_z is calculated by using Equation 15 for experiments of Lu (2008). For comparing with the experiment of Ikeda et al. (1991) whose experimental vegetation density is beyond the applicable scope of Equation 15, K_z is, therefore, obtained as $K_z = 0.09u_*h$ (where u_* is the friction velocity of flow), as suggested by Ikeda et al. (1991).

3.2. Channels With the Submerged Vegetation

Flow structure, the turbulent diffusion, and the dispersion in the submerged vegetated flow are much complicated than that in the emergent vegetated flow (Huai, Chen, et al., 2009; Nepf, 2012). As the expression of the dispersive and diffusion coefficients changes with water depth, Equation 11 needs to be solved at three layers to obtain the solution of SSC.

Table 2
Flow and Sediment Characteristics of Experiments of Lu (2008) and Yuuki and Okabe (2002) in the Submerged Vegetated Flow (k is the von Karman's Constant)

Sources	Run number	H (cm)	h (cm)	D (cm)	d (mm)	s (10^{-3})	u_* (cm/s)	U (cm/s)	k/	a_v (m^{-1})
Lu	C12	12	6.0	0. 6	0.217	4.65	4.76	27.86	0.25	3
	C15	15	6.0	0. 6	0.217	3.50	4.77	29.34	0.27	3
	C18	18	6.0	0. 6	0.217	2.69	5.20	32.12	0.28	3
Yuuki and Okabe	Y1	6	3.5	0.2	0.100	1.00	2.13	22.70	0.20	2.08
	Y2	6	3.5	0.2	0.100	1.50	2.60	28.10	0.20	2.08
	Y3	6	3.5	0.2	0.100	2.00	3.01	31.90	0.20	2.08

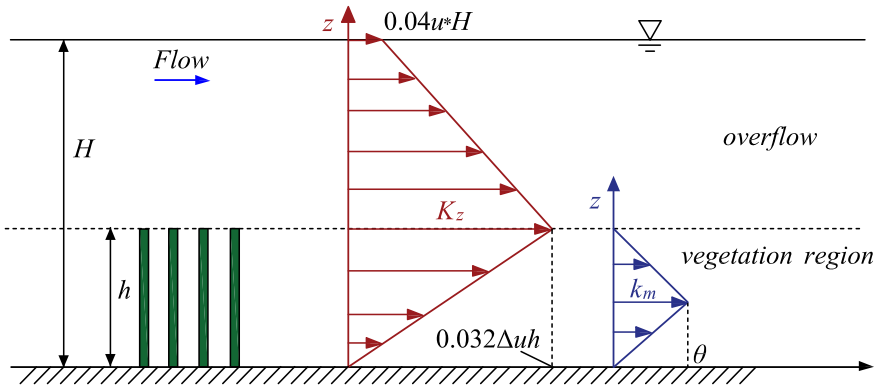

Figure 2. Sketch of the submerged vegetation and the profile of K_z and k_m in the experiment of Lu (2008).

Lu (2008) and Yuuki and Okabe (2002) conducted experiments to study the interaction of the suspended sediment load and vegetation in the submerged vegetated flow. These experiments are used for comparing and validating the present analytical model. Table 2 lists the parameters and measurements of these two experiments. As the construction of experimental vegetation in these two experiments differs greatly from each other, the equations of the turbulent diffusion coefficient are also different, as demonstrated below.

Figure 2 is the sketch of the vertical turbulent diffusion coefficient and the morphological coefficient of the experiments of Lu (2008), in which the vegetation was modeled by rigid straight rods. Based on the study of Nepf (2012), the maximum value of the turbulent diffusion coefficient appears at the top of vegetation for flow with dense vegetation ($a_v h > 0.1$) and can be expressed as

$$K_z(z = h) = 0.032\Delta u h, \tag{17}$$

where Δu represents the velocity difference between the wake region of vegetation and overflow, which is approximately equal to $0.8u_H - u_w$ (where u_H is the flow velocity at the water surface and can be expressed as the logarithmical profile (Huai et al., 2019) and $u_w = \sqrt{2gs/(C_D a_v)}$ is the averaged velocity in the wake region of vegetation and can be obtained according to the balance of gravity and drag (Huai, Chen, et al., 2009). The diffusion coefficient is usually 0 at the channel bed. In addition, in order to avoid the obvious mistake that the SSC is 0 at the water surface caused by the approximation of $K_z(z = H) = 0$, for example, the solution of the classical Rouse equation (Rouse, 1937), the turbulent diffusion coefficient at the water surface of flow cannot be 0. The study of Elder (1959) showed that the depth-averaging turbulent diffusion coefficient is equal to $ku_*H/6$. In this study, the von Karman's constant (see Table 2) is smaller than 0.4, which is the value in clear water flow. For three conditions of Lu (2008), the mean value of the von Karman's constant k approximates to 0.26. Therefore, the expression of K_z is approximated as $K_z(z = H) \approx 0.04u_*H$ at the water surface. The results show that the SSC modeled by this expression is consistent with the experimental observations near the water surface. After obtaining the values of K_z at three locations, namely, the water surface, the top of vegetation, and the channel bed, assuming a linear transition within the region of vegetation and overflow yields the expression of the vertical turbulent diffusion coefficient

$$K_z = \begin{cases} k_2 z + b_2 & z \geq h \\ k_1 z + b_1 & z < h \end{cases}, \tag{18}$$

where the parameters k_1, k_2, b_1, and b_2 differ in different experimental conditions. For experiments of Lu (2008), the parameters are calculated as $k_1 = 0.032\Delta u$, $b_1 = 0$, $k_2 = (0.04u_*H - 0.032\Delta u h)/(H - h)$, and $b_2 = 0.032\Delta u h - k_2 h$. The dispersive coefficient in the vegetation region is simulated by using Equation 13 and is ignored in the overflow where the dispersive term is much smaller than the turbulent diffusion term.

Yuuki and Okabe (2002) carried out experiments in which the vegetation was composed of stagger-arrangement three-layer cylinders with averaged diameter $D = 2$ mm, as shown in Figure 3. The

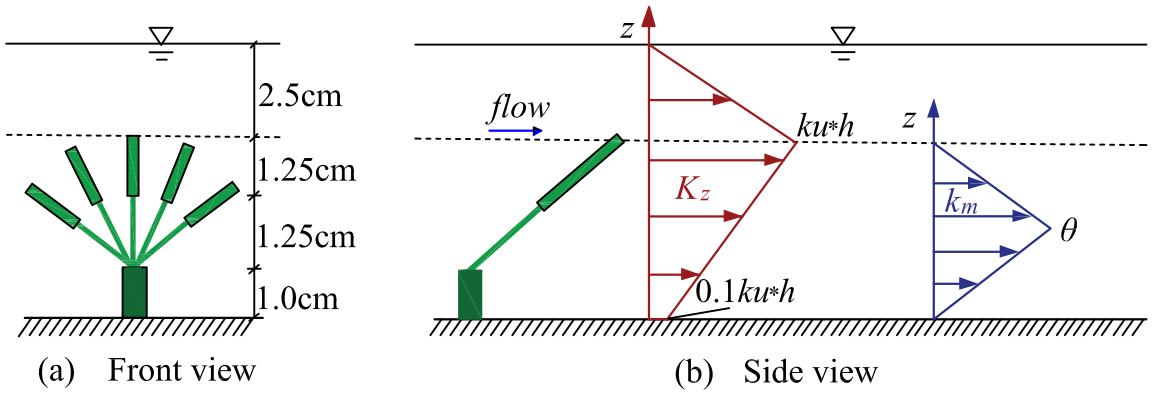

Figure 3. The sketch of the vegetation structure, K_z and k_m in the experiment of Yuuki and Okabe (2002). (a) The front view of the vegetation. (b) The side view of the vegetation, profile of the turbulent diffusion coefficient, and the morphological coefficient.

five branches significantly affect the value of the turbulent diffusion and the dispersive coefficient. Therefore, Equation 17 is not applicable for this experimental condition as it was established based on the experiments with the vegetation of straight rigid rods. However, the turbulent diffusion coefficient can still be divided into two layers according to the height of vegetation and is assumed to be linear profile in each layer (see Figure 3). According to the study of Yang and Choi (2010), the diffusion coefficient at the top of vegetation is $K_z(z = h) = ku_*h$, and $K_z(z = 0) = 0.1ku_*h$ is used at the bottom of channel where the turbulent diffusion coefficient is not 0 according to the experimental observation in Yuuki and Okabe (2002). The four parameters are then calculated as $k_2 = \frac{ku_*h}{h-H}$, $b_2 = -\frac{ku_*hH}{h-H}$, $k_1 = 0.8ku_*$, and $b_1 = 0.1ku_*h$, respectively. The referenced level $z_a = H/2$ is also used for open channel flows with the submerged vegetation.

The analytical solution of Equation 11 associated with various $K_z(z)$ and k_m can then be obtained in three layers with some differences for these two experiments of different conditions, as described below.

For experiments of Lu (2008), the referenced height is in the overflow region, that is, $z_a \geq h$. In the overflow region ($z \geq h$), the effect of the vegetation-induced dispersion is assumed to be small and can be ignored. Substituting Equations 18 and 13a into Equation 11, solving the ordinary differential equation obtains the SSC in the overflow region in the uniform submerged vegetated flow:

$$C(z) = C(z_a)\left(\frac{k_2 z + b_2}{k_2 z_a + b_2}\right)^{-\frac{\omega}{k_2}}. \tag{19}$$

In the upper vegetation region, that is, $h/2 \leq z < h$, the analytical solution of Equation 11 with consideration of the dispersion term is

$$C(z) = C(h)\exp\left(\frac{r_1}{k_1}(z-h)\right)\left(\frac{k_1 z + b_1}{k_1 h + b_1}\right)^{\frac{\lambda_1 k_1 - r_1 b_1}{k_1^2}}, \tag{20}$$

where $r_1 = 2\theta K_f U/h$, $\lambda_1 = -2\theta K_f U - \omega$, and $C(h)$ denotes the SSC at the top of vegetation and can be calculated by Equation 19 as follows:

$$C(h) = C_a\left(\frac{k_2 h + b_2}{k_2 z_a + b_2}\right)^{-\frac{\omega}{k_2}}. \tag{21}$$

The analytical solution of SSC in the lower vegetation region (i.e., $z < h/2$) is

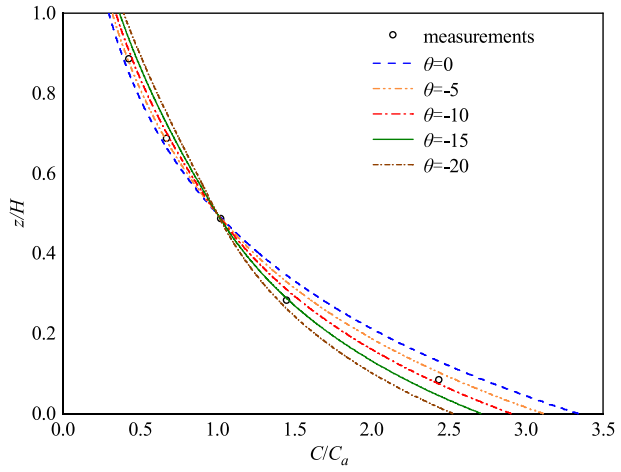

Figure 4. Comparison of the vertical SSC profiles of the predicted (lines for different morphological conditions) by Equations 16a and 16b and measured (open circles, Ikeda et al., 1991).

$$C(z) = C\left(\frac{h}{2}\right)\exp\left(\frac{r_2}{k_1}\left(z-\frac{h}{2}\right)\right)\left(\frac{k_1 z+b_1}{k_1\frac{h}{2}+b_1}\right)^{\frac{\lambda_2 k_1 - r_2 b_1}{k_1{}^2}}, \quad (22)$$

where $r_2 = -2\theta K_f U/h$, $\lambda_2 = -\omega$, and $C(h/2)$ represents the SSC at the half height of vegetation and can be calculated by Equation 20.

In the experiments of Yuuki and Okabe (2002), the referenced height is within the vegetation region, that is, $h/2 < z_a = H/2 < h$. Therefore, the analytical solution of the profile of SSC differs from above. In the upper vegetation region, that is, $h/2 \le z \le h$, the analytical solution of Equation 11 with consideration of the dispersion term is

$$C(z) = C(z_a)\exp\left(\frac{r_1}{k_1}(z-z_a)\right)\left(\frac{k_1 z+b_1}{k_1 z_a+b_1}\right)^{\frac{\lambda_1 k_1 - r_1 b_1}{k_1{}^2}}. \quad (23)$$

In the overflow region ($z > h$), the effect of vegetation-induced dispersion is assumed to be small and can be ignored. Substituting Equations 18 and 13a into Equation 11, and solving Equation 11 yields SSC:

$$C(z) = C(h)\left(\frac{k_2 z+b_2}{k_2 h+b_2}\right)^{-\frac{\omega}{k_2}}, \quad (24)$$

where $C(h)$ can be calculated by Equation 23.

The analytical solution of SSC in the lower vegetation region (i.e., $z < h/2$) is

$$C(z) = C\left(\frac{h}{2}\right)\exp\left(\frac{r_2}{k_1}\left(z-\frac{h}{2}\right)\right)\left(\frac{k_1 z+b_1}{k_1\frac{h}{2}+b_1}\right)^{\frac{\lambda_2 k_1 - r_2 b_1}{k_1{}^2}}, \quad (25)$$

where $C(h/2)$ represents the SSC at the half height of vegetation and can be calculated by Equation 23.

4. Results

4.1. Emergent Vegetation

Figures 4 and 5 show the comparison of the predicted and measured vertical profiles of SSC for experiments of Ikeda et al. (1991) and Lu (2008), respectively. It is seen that the analytical solution ignoring the dispersive term, that is, $\theta = 0$ (blue dashed lines in Figures 4 and 5), greatly underpredicts SSC above the half height of flow depth and significantly overpredicts SSC within half height of flow depth. This indicates that the effect of the dispersive flux on the vertical SSC distribution in the vegetated open channel flows is significant and cannot be ignored in calculating the vertical SSC profile. It is seen from Figures 4 and 5 that the dispersive coefficient is usually negative, which means that the direction of the dispersive flux is opposite to the settling flux. According to the mass conservation, the total upward flux, that is, the sum of the diffusion flux and the dispersive flux, has to balance with the settling flux. Therefore, the opposite dispersive flux weakens the effect of the settling flux on the total vertical SSC profile. In addition, the SSC decreases in the region near the river bed and increases in the region near the water surface with the increase of the absolute value of the dispersive coefficient. However, when the absolute value of the dispersive coefficient is very large, the deviation between the predicted and measured SSC becomes larger again, while the sediment concentration changes from overpredicted to underpredicted within the half height of the flow depth.

In Figure 5, values of H and a_v for different experiments are shown in the figure for convenience of comparison. Results with the same vegetation density but different flow depths (i.e., Figures 5a, 5d, and 5g, Figures 5b, 5e, and 5h, and Figures 5c, 5f, and 5i) show that the relationship between the dispersive coefficient and flow depth is not very clear. However, the comparison of the same flow depth but different

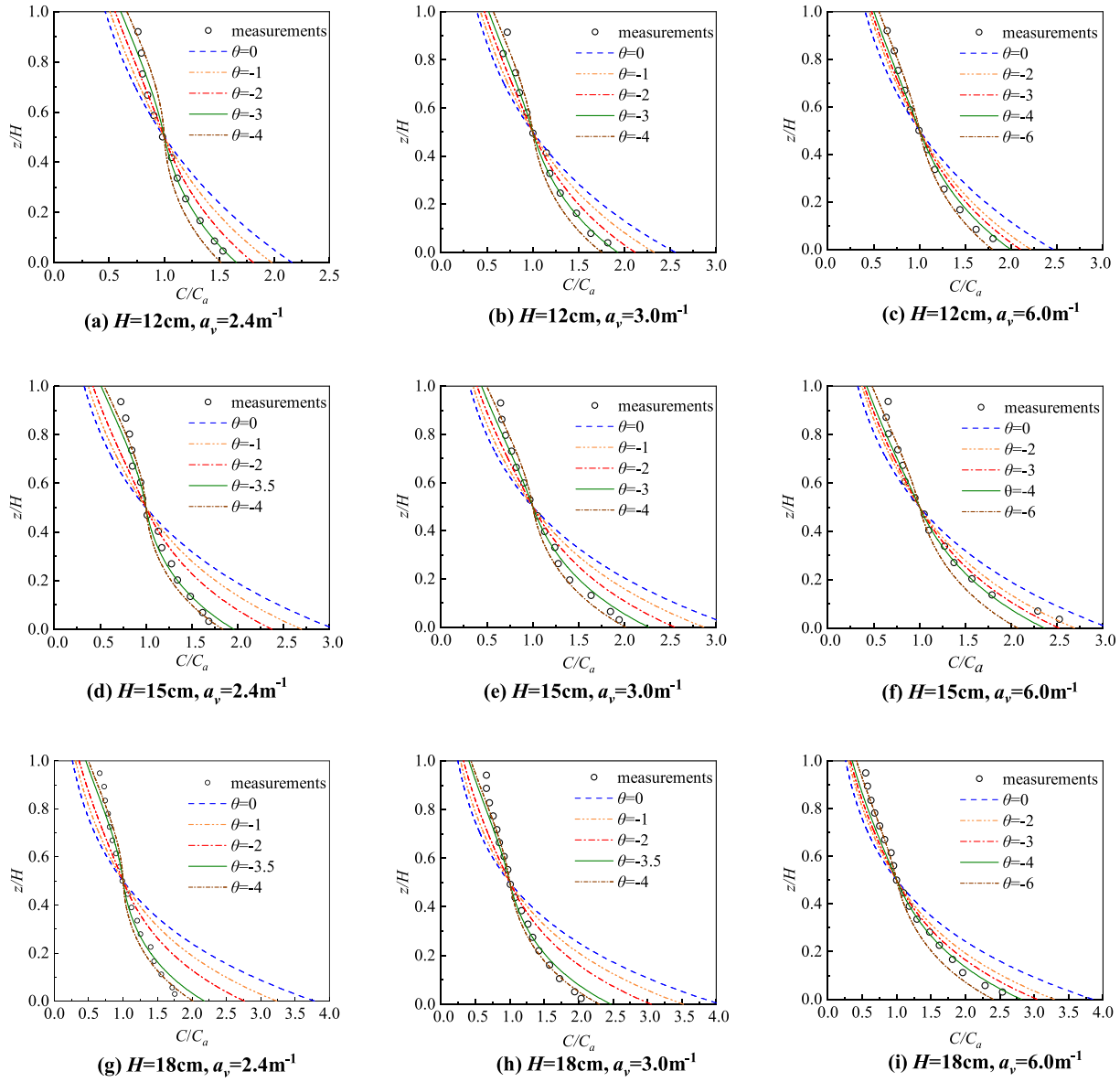

Figure 5. Comparison of the vertical SSC profiles of the predicted (lines for different morphological conditions) by Equations 16a and 16b and experimentally measured (open circles, Lu, 2008) for different vegetation heights and densities. As shown in figure: (a) D12-1, (b) D12-2, (c) D12-3, (d) D15-1, (e) D15-2, (f) D15-3, (g) D18-1, (h) D18-2, and (i) D18-3.

vegetation densities, that is, Figures 5a–5c, 5d–5f, and 5g–5i, shows that the vegetation density has significant impact on the dispersive coefficient. Specifically, the maximum absolute values of the averaged fitting morphological coefficient are −10, −3.7, −3.5, and −4, corresponding respectively to the vegetation density of 1, 2.4, 3, and 6 m^{-1}. In general, Figure 5 demonstrates that the absolute value of the morphological coefficient decreases with the increase of the vegetation density with the exception of the case $a_v = 6\ m^{-1}$. This exception case may be ascribed to the following fact: In the experiment of Lu (2008), the arrangement of the vegetation was regular, and in the cases of D12/D15/D18-3, that is, $a_v = 6\ m^{-1}$, the transverse and longitudinal interval between the vegetation centers was, respectively, 2 and 5 cm. For this exception case, that is, $a_v = 6\ m^{-1}$, the ratio of the transverse interval over the longitudinal interval was 0.4, while this ratio was approximate to one in the cases of $a_v = 1$, 2.4, and 3 m^{-1}. However, the conclusions of the dispersive rules and empirical coefficient α of Equation 15 are obtained from the experiments of stagger arrangement where the ratio of the transverse interval over the

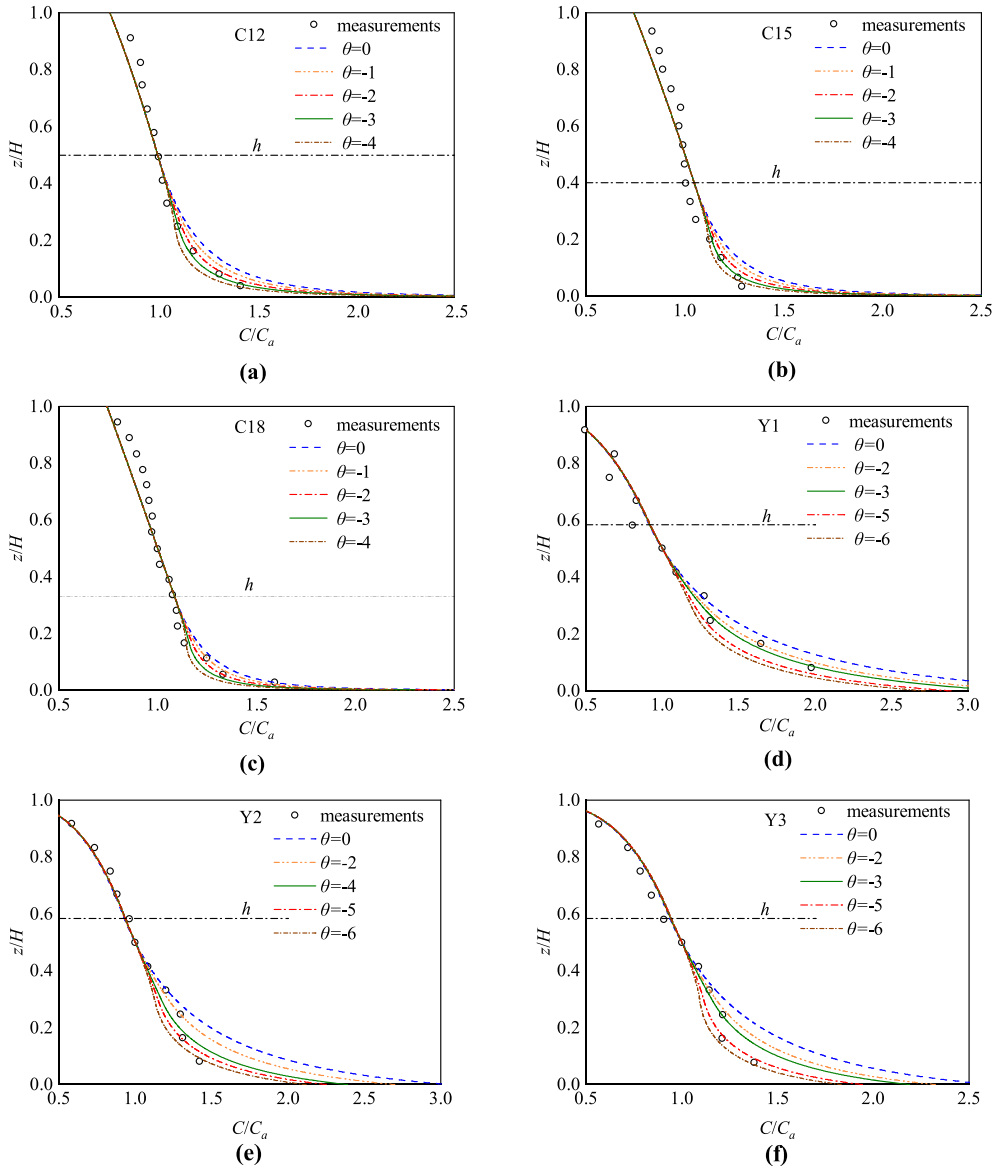

Figure 6. The comparison between analytically predicted (lines) and experimentally measured (Lu, 2008; Yuuki & Okabe, 2002: open circles) vertical SSC profile in the submerged vegetated flow. The dash-dotted lines in the figures show the height of vegetation for the conditions. As shown in the figure: (a) C12, (b) C15, (c) C18, (d) Y1, (e) Y2, and (f) Y3.

longitudinal interval is approximate to one. From this aspect, the unusual result for condition $a_v = 6\,\mathrm{m}^{-1}$ may be caused by the arrangement of vegetation, which requires further experimental study for confirmation.

4.2. Submerged Vegetation

Figure 6 shows the comparison of the predicted and measured vertical SSC profiles in the submerged vegetated open channel flows. In the experiments of Lu (2008), the ratio of the flow depth over the vegetation height varies, while the vegetation density is fixed (see Table 2 for details of the flow conditions). Figures 6a–6c show that the deviation of the predicted SSC from the measured SSC decreases with the increase of the vegetation submergence for the condition without the dispersive term (i.e., blue dashed lines). This indicates that the effect of the vegetation on the vertical SSC profile is weakened with the increase of the vegetation submergence (i.e., H/h increases). This may be because the relative importance of the vegetation drag over the bed friction drag decreases for high vegetation submergence (Nepf, 2012;

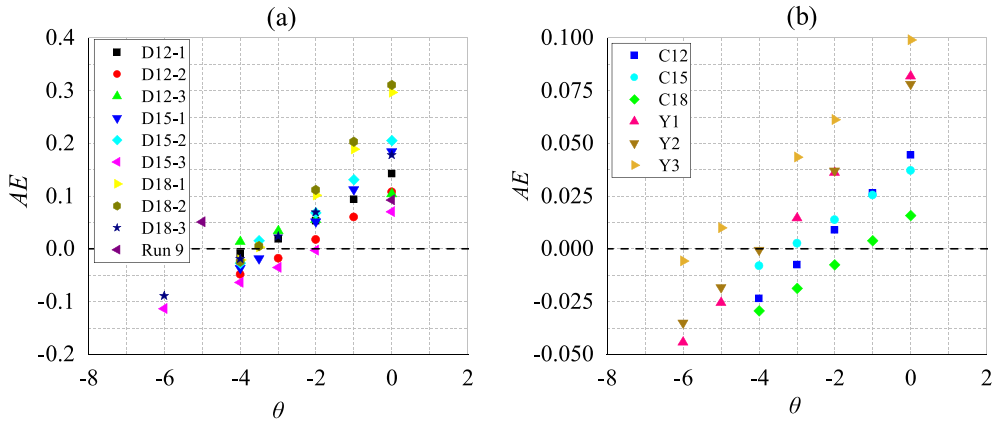

Figure 7. The variation of the vertical averaged error between the predicted and observed SSC with θ. (a) The emergent vegetated open channel flow and (b) the submerged vegetated open channel flow.

Nepf & Vivoni, 2000; Raupach et al., 1996). Figures 6a–6c show that $\theta = -3$ (i.e., green solid lines) better represents the vegetation-induced dispersive coefficient, indicating that the dispersive coefficient has little relationship with the vegetation submergence for the flow conditions of Lu (2008).

The values of the dispersive coefficient for the experiments of Yuuki and Okabe (2002) are slightly larger than the values in the experiments of Lu (2008). This may be ascribed to the fact that the vegetation structure in the experiments of Yuuki and Okabe (2002) favors the dispersion. It is seen from Figure 6d that the vertical SSC profile can be reasonably predicted with the dispersive coefficient $\theta = -3$, while Figures 6e and 6f show that some deviations exist between the predicted and the measured SSC. This may be due to the complicated vegetation structure in their experiments, indicating that the analytical model proposed in this study has some defects and cannot provide accurate prediction of the SSC in such complicated vegetation structure. Nevertheless, the predicted SSC for the experiments of Yuuki and Okabe (2002) is much better than the previous similar study (see Figure 10 in Yang & Choi, 2010), which did not consider the effect of the dispersive term.

Analysis of the results shows that the analytical solution agrees well with experimental measurements in the region of overflow. For regular arrangement of straight cylinders (i.e., the experiments of Lu, 2008), $a_v = 3\ \mathrm{m}^{-1}$, the vertical SSC profile within the vegetation region can be accurately predicted using the analytical approach proposed in this study with an appropriate dispersive coefficient. For the staggered vegetation with complicated structure (i.e., the experiments of Yuuki & Okabe, 2002), $a_v = 2.08\ \mathrm{m}^{-1}$, some deviation between the analytical prediction and the measurement exists within the vegetation region. The variation of the vertical SSC profile with the dispersive coefficient found in the emergent vegetated flow also appears in the submerged vegetated flow; that is, the SSC decreases with the increase of the absolute value of the dispersive coefficient in the vegetated region.

4.3. Analysis

Result of Figures 4–6 shows that the analytical solutions either overpredict or underpredict the SSC at different regions of the vegetated open channel sediment-laden flow. In order to represent the deviation of the predicted SSC from the observed SSC for different values of θ, the averaged error (AE) is defined as follows:

$$AE = \frac{\sum \left(C_{\mathrm{pre}} - C_{\mathrm{obs}}\right)}{N}, \tag{26}$$

where N is the sampling number of the observed SSC in the vertical direction at a monitoring position in the experiments, C_{obs} is the observed SSC, and C_{pre} represents the predicted SSC by the proposed model.

In order to determine the best fitted value of θ, another common statistical parameter, that is, the mean relative error (MRE), is also used to evaluate the error of the proposed model:

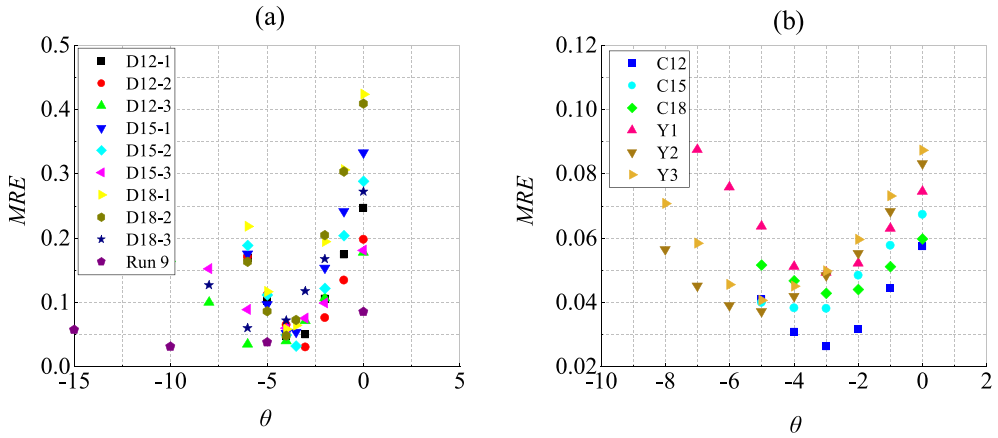

Figure 8. The variation of the *MRE* with θ: (a) the emergent vegetated open channel flow and (b) the submerged vegetated open channel flow.

$$MRE = \frac{\sum \frac{|C_{pre} - C_{obs}|}{C_{obs}}}{N}. \quad (27)$$

Figure 7 shows the relationship between the *AE* and θ for both the emergent and the submerged vegetated open channel flow, which clearly demonstrates whether the model overpredicts or underpredicts SSC. It is seen from Figure 7 that the SSC is usually overpredicted by the proposed model (the positive value of *AE*) for the $\theta = 0$. With the increase of the absolute value of θ, the SSC simulated by the proposed model varies from the overpredicted to the underpredicted (the negative value of *AE*) for both the submerged and the emergent vegetated open channel flow. The scope of θ corresponding to $AE = 0$ in the emergent vegetated open channel flow is much more centralized than that in the channel with the submerged vegetation. The specific best fitted value of θ can be determined by the variation of *MRE* calculated by Equation 27.

Figure 8 is the variation of *MRE* with θ for open channel flow with both the emergent (Figure 8a) and the submerged (Figure 8b) vegetation, respectively. Figure 8 shows that *MRE* decreases firstly and then increases with the increase of θ. The value of θ corresponding to the smallest *MRE* is known as the best fitted value for that condition, which is listed in the last column of Table 3. Small *MRE* indicates that the model proposed in this study can accurately simulate the vertical profile of SSC in the vegetated open channel flow. The suggested value of θ is from -5 to -3 for the channels with the range of vegetation density a_v being from 2 to 6 m^{-1}. More specifically, the best fitted value of θ approximates to -4 with the range of the vegetation density being from 2 to 6 m^{-1} in the open channel flow with the emergent vegetation. More experiments and studies are required to explore the rules of the dispersive coefficient in the open channel flow with the vegetation density outside the scope of $2\ m^{-1} < a_v < 6\ m^{-1}$.

Table 3
The Parameters and the Best Fitted Value of θ for Open Channel Flow With the Emergent and the Submerged Vegetation

Conditions	Run number	Re_s	$a_v\ (m^{-1})$	θ
Emergent vegetation	D12-1	1,994	2.4	−3
	D12-2	1,740	3	−3
	D12-3	1,008	6	−4
	D15-1	1,981	2.4	−4
	D15-2	1,749	3	−3.5
	D15-3	1,014	6	−4
	D18-1	2,049	2.4	−4
	D18-2	1,758	3	−4
	D18-3	1,009	6	−4
	Run 9	1,420	1	−10
Submerged vegetation	C12	991	3	−3
	C15	859	3	−3
	C18	753	3	−3
	Y1	153	2.08	−3
	Y2	187	2.08	−4
	Y3	217	2.08	−5

Above discussion shows that the magnitude of the dispersive coefficient is mainly influenced by the flow field (mainly velocity) and the vegetation characteristics (density and structure). The flow field can be represented by using the stem Reynolds number, that is, $Re_s = \frac{u_w D}{\nu}$. The complicated vegetation structure enhances the dispersive strength through influencing the flow turbulence and the spatial heterogeneity, which can be proved by comparing the values of θ between the experiments of Yuuki and Okabe (2002) and the experiments of Lu (2008). Table 3 lists the stem Reynolds number, the

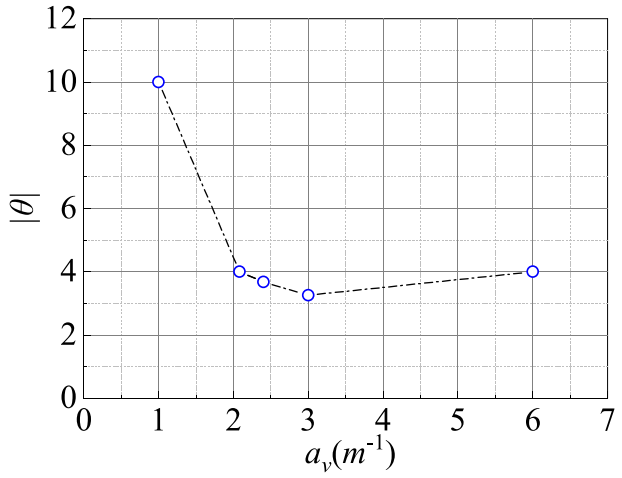

Figure 9. The variation of the absolute value of the maximum morphological (dispersive) coefficients with the vegetation density.

vegetation density, and the best fitted θ. The vegetation density for the experiments of Yuuki and Okabe (2002) (i.e., Conditions Y1, Y2, and Y3) is all 2.08, while the stem Reynolds number increases gradually. Therefore, the results of Y1, Y2, and Y3 indicate that the dispersion increases with the increase of Re_s, which may be caused by the strong turbulence induced by the large stem Reynolds number and corresponding intensive spatial heterogeneity. The value of θ for the Experiments C12, C15, and C18 is all −3, while the stem Reynolds number varies slightly. This phenomenon may be ascribed to the fact that the vegetation structure of C12, C15, and C18 is regular and variation of the stem Reynolds number is small.

For both the emergent and the submerged vegetated open channel flow investigated in this study, Figure 9 shows that the averaged absolute value of θ decreases with the increase of the vegetation density, where θ is obtained by averaging the value of θ for the conditions of the same vegetation density. The results show that the gradient of the morphological coefficient with the vegetation density is large for the condition $a_v < 2.08\ \mathrm{m}^{-1}$, while the gradient is small for dense vegetation conditions investigated in this study. Within the vegetation region, the stem wakes become a localized source of turbulence such that the turbulent flow field is much more heterogeneous than that in the region without vegetation (Nepf et al., 1997). Thus, the dispersive coefficient is significantly increased by the presence of vegetation for small vegetation density. The interval between the vegetation stem's centers decreases gradually with the increase of the vegetation density, leading to the decrease of characteristic area of spatial averaging. Therefore, the vegetation-induced vortices may overlap in the characteristic area, which weakens the local inhomogeneity, and thus, the dispersive coefficient decreases. Figure 9 also shows that the dispersive coefficient increases again when the vegetation density increases to $a_v = 6\ \mathrm{m}^{-1}$. This could be caused by the arrangement of vegetation for the case of $a_v = 6\ \mathrm{m}^{-1}$. More experiments are needed for better understanding and interpretation of the phenomenon.

5. Discussion

The simulation of SSC in the vegetated open channel sediment-laden flow is very complicated. It requires well-defined flow field including flow velocity and turbulence strength, as well as the sediment particle characteristics. The empirical equations of the vertical turbulent diffusion coefficient used for conditions of Lu (2008) are obtained from the previous flume experiments (Nepf, 1999, 2004, 2012), which are interpreted as that the same straight rigid rods are used as the experimental vegetation and the vegetation density is within the scope of these formulas. For other conditions used in this study, experimental conditions are outside the scope of these formulas. As such, the turbulent diffusion coefficient has to be determined by the corresponding experimental observations or previous studies (Yang & Choi, 2010). The model proposed in this study is based on the correct determination of the turbulent diffusion coefficient model. Therefore, it is still a challenge task to extend the present model to open channel flow with the natural live (flexible) vegetation. Nevertheless, the proposed model is a simple and effective tool for simulating the vertical profile of SSC in the open channel flow with vegetations.

The double-averaging method, in which the classical time-averaging advection-diffusion equations are averaged over spatial area in the plane parallel to the bottom of channel, is used to simulate the vertical SSC profile in the vegetated open channel flow. The application of the double-averaging method for flow field analysis reduces the discordance resulted from the spatial heterogeneity within the vegetation region. In order to solve the double-averaging advection-diffusion equations, the diffusive flux is expressed by the Fickian diffusion model, while the dispersive flux is the product of the dispersive coefficient K_D and the mass flux CU. According to the previous experiments and the results of this study, the proposed dispersive model generalizes the influences of the dispersion as the function of coordinate z. As such, the size of the spatial averaging is not emphasized in this study. The suggestion about the size of the spatial averaging is that it must represent the spatial heterogeneity to reduce the error induced by the variation of the

spatial-averaging size. For example, it is correct to use the whole domain parallel to the bed as the size of the spatial averaging for open channel flow with irregular staggered vegetation or rough bed (Nikora, McLean, et al., 2007). For open channel flow with regular staggered vegetation, the region of the adjacent four vegetations is suggested as the size of the spatial averaging (Poggi, Katual, & Albertson, 2004; Yuuki & Okabe, 2002).

There is little knowledge about the dispersive coefficient model, while most previous investigations focused on the dispersive stress obtained from the experimental measurements. Experiments with natural vegetation (*Salix pentandra*) showed that the distribution of the dispersive stress is very complicated (Righetti, 2008) in which the magnitude of the dispersive stress at the top of vegetation and river bed is smaller than that at the half height of vegetation. Coceal et al. (2008) and Poggi and Katul (2008b) carried out experiments using rigid straight vegetation. Their results showed that the maximum value of the dispersive stress occurred at almost the half height of vegetation and decreased toward both up and down vertical directions. The results also showed that the magnitude of the dispersive stress greatly depended on the vegetation density. Based on these laboratory experimental studies, the authors assume that the variation of the dispersive flux, that is, $\langle u_3\,''c''\rangle = -K_D UC$, in the vegetated open channel flow is similar to that of the dispersive stress. For simplification, the authors further assume that the dispersive coefficient K_D is a triangle profile in the vegetation region as expressed in Equations 12 and 13. The comparison of the SSC profile simulated by proposed model with the experimental measurements confirms the strong relation between dispersive coefficient and the vertical SSC profile in the vegetated open channel flows.

Results show that the dispersive term (usually appearing as negative value) plays an important role in determining the vertical SSC profile in the vegetated suspended sediment-laden flow. For the emergent vegetated flow, the model calculated SSC from the half height of the vegetation to the channel bottom varies from overprediction to underprediction with the increase of the absolute value of the dispersive coefficient, while the predicted SSC above the half height of vegetation has opposite variation trend (see Figures 4 and 5). For the submerged vegetated flow, the variation of SSC within the vegetation region is similar to that under the half height of vegetation of the emergent vegetated flow (see Figure 6). This means that the appropriate dispersive coefficient can be obtained by fitting the experimental data. Because all the dispersive coefficients are modeled as triangle profile, the maximum value of the morphologic coefficient (i.e., θ) is used to represent the magnitude of the dispersive coefficient. The relationship between the best fitted value of θ and the vegetation density, the vegetation structure, and the stem Reynolds number depends on the experimental conditions. This means that the best fitted values of θ proposed in this paper can only represent the conditions investigated in this study. However, the rules between θ and a_v, Re_s, and the vegetation structure conform to the physical mechanism and are strongly supported by previous relevant experimental studies.

6. Conclusions

In this paper, the model of the dispersive coefficient is proposed based on the concept of the dispersion to investigate the vertical SSC profile in the vegetated suspended sediment-laden flow. The double-averaging method is applied to simulate the vertical SSC profile in the vegetated open channel flow with time-spatial averaging advection-diffusion equations. The proposed model is validated by comparing the analytical solution of the vertical SSC profile with the existing experimental measurements. Results show that the proposed model of the dispersive coefficient is reliable and can be used to estimate the vertical SSC profile in the complicated vegetated, sediment-laden open channel flow. The following conclusions can be drawn from this study.

1. A model for estimating the dispersive coefficient is proposed in this study based on the concept of the dispersion. For both the emergent and the submerged vegetated open channel flow investigated in this study, the dispersive coefficient decreases with the increase of the vertical axis z from the half height of the vegetation and increases with the increase of z from the channel bottom to the half height of vegetation. The dispersive coefficient reaches 0 at both the top of the vegetation and the channel bottom.
2. The effect of the dispersion on the vertical SSC profile within the vegetation region is significant and cannot be ignored. The inclusion of the dispersive term can greatly improve the prediction of the vertical SSC profile in the vegetated region and the region close to the channel bottom. The dispersive term can be

extended to the roughness bed or rivers with sand ripples, where the spatial heterogeneity of flow structure is also strong owing to the complicated uneven channel morphology.

3. The double-averaging method is applied to simulate the vertical SSC profile in the vegetated open channel flow for improving the prediction of SSC. This is particularly important in the region of vegetation, where the spatial heterogeneity of the turbulent flow is strong owing to the presence of vegetation.
4. The fitted morphological coefficient is mainly related to the vegetation density, the flow field, and the vegetation structure in this study. For the conditions investigated in this study, the absolute values of the morphological and the dispersive coefficients decrease sharply with the increase of vegetation density, then increase slightly with the increase of vegetation density.
5. The suggested range of θ is -5 to -3 with the mean-related error smaller than 10% when the vegetation density a_v is within the range from 2 to 6 m^{-1}. Owing to the limited available experimental data, it is not clear what is the variation trend of the dispersive coefficient for sparse vegetation density (i.e., $a_v < 1\ m^{-1}$) and very dense vegetation density (i.e., $a_v > 6\ m^{-1}$). Further experiments with a wide range of the vegetation density are required to accurately propose the dispersive model.

Nomenclature

A	integral constant
a_v	the frontal area density of vegetation
b_1, b_2	parameters of expression of turbulent diffusion coefficient profile at region $z < h$ and $z \geq h$ respectively in submerged vegetated open channel flows
C	time-spatial averaging suspended sediment concentration
C_a	referenced suspended sediment concentration at referenced height
C_D	drag coefficient of vegetation
C_{pre}	predicted suspended sediment concentration by this model
C_{obs}	observed suspended sediment concentration in experiments
c	instantaneous suspended sediment concentration
D	diameter of vegetation
d	representative size of sediment particles
f, φ	two different variables
g	acceleration of gravity
H	flow depth
h	height of vegetation
K_D	dispersive coefficient
K_f	a scale factor and $K_f = 0.001$ in present study
K_m	molecular diffusion coefficient
K_z	vertical turbulent diffusion coefficient
k	von Karman's constant
k_1, k_2	gradients of expression of turbulent diffusion coefficient profile at region $z < h$ and $z \geq h$ respectively in submerged vegetated open channel flows
k_m	morphological coefficient
N	sampled number of the observed SSC in the vertical direction at a monitor point in the experiments
n	number of vegetation per unit area
r_1, λ_1	two parameters
Re_s	stem Reynolds number
r_2, λ_2	two parameters
S	source or sink of sediment in advection-diffusion equation
s	slope of channel bed
t	time
U	averaged longitudinal flow velocity of cross section
u	instantaneous longitudinal flow velocity

u_*	friction velocity
u_w	averaged velocity in the wake region of vegetation
u_H	flow velocity at the water surface
u_j	instantaneous flow velocity component in jth direction
u_1, u_2, u_3	instantaneous flow velocity of longitudinal, transverse, and vertical, respectively
x_j	the jth direction, $x_1 = x$, $x_2 = y$, and $x_3 = z$ are directions of longitudinal, transverse, and vertical, respectively
z	vertical coordinate
z_a	referenced height
α	a proportional factor
γ_f	the bulk density of water
γ_s	the bulk density of sediment
σ	a constant
υ	the kinematic viscosity of water
ω	settling velocity of sediment particles
θ	values of morphological coefficient at the half height of vegetation
$\triangle u$	velocity difference between the region of vegetation wake and overflow
$'$	the deviation of instantaneous variables from time-averaging variables
$''$	the deviations of time-averaged variables from spatial-averaged variables
$\bar{}$	time average
$< >$	spatial average
$<\bar{}>$	time-spatial average

Conflict of Interest

There are no real or perceived financial conflicts of interests for any author and no other affiliations for any author that may be perceived as having a conflict of interest with respect to the results of this paper.

Data Availability Statement

All the data used in this work have been reported elsewhere (Ikeda et al., 1991; Lu, 2008; Yuuki & Okabe, 2002).

Acknowledgments
The research reported here is financially supported by the Natural Science Foundation of China (11872285 and 11672213), the U.K. Royal Society-International Exchanges Program (IES\R2\181122), and the Open Funding of State Key Laboratory of Water Resources and Hydropower Engineering Science (WRHES), Wuhan University (Project 2018HLG01). Comments made by reviewers have greatly improved the quality of the final paper.

References

Boudreault, L., Dupont, S., Bechmann, A., & Dellwik, E. (2017). How forest inhomogeneities affect the edge flow. *Boundary-Layer Meteorology*, *162*(3), 375–400. https://doi.org/10.1007/s10546-016-0202-5

Coceal, O., Thomas, T. G., & Belcher, S. E. (2007). Spatial variability of flow statistics within regular building arrays. *Boundary-Layer Meteorology*, *125*(3), 537–552. https://doi.org/10.1007/s10546-007-9206-5

Coceal, O., Thomas, T. G., & Belcher, S. E. (2008). Spatially-averaged flow statistics within a canopy of large bluff bodies: Results from direct numerical simulations. *Acta Geophysica*, *56*(3), 862–875. https://doi.org/10.2478/s11600-008-0025-y

Coceal, O., Thomas, T. G., Castro, I. P., & Belcher, S. E. (2006). Mean flow and turbulence statistics over groups of urban-like cubical obstacles. *Boundary-Layer Meteorology*, *121*(3), 491–519. https://doi.org/10.1007/s10546-006-9076-2

Elder, J. W. (1959). The dispersion of marked fluid in turbulent shear flow. *Journal of Fluid Mechanics*, *5*(04), 544–560. https://doi.org/10.1017/S0022112059000374

Florens, E., Eiff, O., & Moulin, F. (2013). Defining the roughness sublayer and its turbulence statistics. *Experiments in Fluids*, *54*(4), 1500. https://doi.org/10.1007/s00348-013-1500-z

Fu, X. D., Wang, G. Q., & Shao, X. (2005). Vertical dispersion of fine and coarse sediments in turbulent open-channel flows. *Journal of Hydraulic Engineering*, *10*(131), 877–888. https://doi.org/10.1061/(ASCE)0733-9429(2005)131:10(877)

Han, X., He, G. J., & Fang, H. W. (2017). Double-averaging analysis of turbulent kinetic energy fluxes and budget based on large-eddy simulation. *Journal of Hydrodynamics*, *29*(4), 567–574. https://doi.org/10.1016/S1001-6058(16)60769-2

Huai, W. X., Chen, Z. B., Han, J., Zhang, L. X., & Zeng, Y. H. (2009). Mathematical model for the flow with submerged and emerged rigid vegetation. *Journal of Hydrodynamics*, *21*(5), 722–729. https://doi.org/10.1016/S1001-6058(08)60205-X

Huai, W. X., Yang, L., Wang, W. J., Guo, Y. K., Wang, T., & Cheng, Y. G. (2019). Predicting the vertical low suspended sediment concentration in vegetated flow using a random displacement model. *Journal of Hydrology*, *578*, 124101. https://doi.org/10.1016/j.jhydrol.2019.124101

Huai, W. X., Zeng, Y. H., Xu, Z. G., & Yang, Z. H. (2009). Three-layer model for vertical velocity distribution in open channel flow with submerged rigid vegetation. *Advances in Water Resources*, *32*(4), 487–492. https://doi.org/10.1016/j.advwatres.2008.11.014

Ikeda, S., Izumi, N., & Ito, R. (1991). Effects of pile dikes on flow retardation and sediment transport. *Journal of Hydraulic Engineering*, *11*(117), 1459–1478. https://doi.org/10.1061/(ASCE)0733-9429(1991)117:11(1459)

Kim, H. S., Kimura, I., & Park, M. (2018). Numerical simulation of flow and suspended sediment deposition within and around a circular patch of vegetation on a rigid bed. *Water Resources Research*, *54*, 7231–7251. https://doi.org/10.1029/2017WR021087

Kundu, S. (2019). Modeling stratified suspension concentration distribution in turbulent flow using fractional advection–diffusion equation. *Environmental Fluid Mechanics*, *19*(6), 1557–1574. https://doi.org/10.1007/s10652-019-09679-9

Le Bouteiller, C., & Venditti, J. G. (2015). Sediment transport and shear stress partitioning in a vegetated flow. *Water Resources Research*, *51*, 2901–2922. https://doi.org/10.1002/2014WR015825

Li, D., Yang, Z. H., Sun, Z., Huai, W. X., & Liu, J. (2018). Theoretical model of suspended sediment concentration in a flow with submerged vegetation. *Water*, *10*(11), 1656. https://doi.org/10.3390/w10111656

Li, S., & Katul, G. (2019). Cospectral budget model describes incipient sediment motion in turbulent flows. *Physical Review Fluids*, *4*, 093801. https://doi.org/10.1103/PhysRevFluids.4.093801

Li, S., Katul, G., & Huai, W. (2019). Mean velocity and shear stress distribution in floating treatment wetlands: An analytical study. *Water Resources Research*, *55*, 6436–6449. https://doi.org/10.1029/2019WR025131

Li, S., Shi, H., Xiong, Z., Huai, W., & Cheng, N. (2015). New formulation for the effective relative roughness height of open channel flows with submerged vegetation. *Advances in Water Resources*, *86*, 46–57. https://doi.org/10.1016/j.advwatres.2015.09.018

Lu, S. Q. (2008). Experimental study on suspended sediment distribution in flow with rigid vegetation (Doctoral dissertation). Hohai University, Nanjing, Jiangsu, China (in Chinese).

Moltchanov, S., Bohbot, R. Y., Duman, T., & Shavit, U. (2015). Canopy edge flow: A momentum balance analysis. *Water Resources Research*, *51*, 2081–2095. https://doi.org/10.1002/2014WR015397

Nepf, H. M. (1999). Drag, turbulence, and diffusion in flow through emergent vegetation. *Water Resources Research*, *35*(2), 479–489. https://doi.org/10.1029/1998WR900069

Nepf, H. M. (2004). Vegetated flow dynamics. In S. Fagherazzi, M. Marani, & L. K. Blum (Eds.), *The ecogeomorphology of tidal marshes*, (Vol. 59, pp. 137–163). Washington, DC: American Geophysical Union. https://doi.org/10.1029/CE059p0137

Nepf, H. M. (2012). Flow and transport in regions with aquatic vegetation. *Annual Review of Fluid Mechanics*, *44*(1), 123–142. https://doi.org/10.1146/annurev-fluid-120710-101048

Nepf, H. M., Sullivan, J. A., & Zavistoski, R. A. (1997). A model for diffusion within emergent vegetation. *Limnology and Oceanography*, *42*(8), 1735–1745. https://doi.org/10.4319/lo.1997.42.8.1735

Nepf, H. M., & Vivoni, E. R. (2000). Flow structure in depth-limited, vegetated flow. *Journal of Geophysical Research*, *105*(C12), 28,547–28,557. https://doi.org/10.1029/2000jc900145

Nikora, V., McEwan, I., McLean, S., Coleman, S., Pokrajac, D., & Walters, R. (2007). Double-averaging concept for rough-bed open-channel and overland flows: Theoretical background. *Journal of Hydraulic Engineering*, *133*(8), 873–883. https://doi.org/10.1061/(ASCE)0733-9429(2007)133:8(873)

Nikora, V., McLean, S., Coleman, S., Pokrajac, D., McEwan, I., & Campbell, L. (2007). Double-averaging concept for rough-bed open-channel and overland flows: Applications. *Journal of Hydraulic Engineering*, *133*(8), 884–895. https://doi.org/10.1061/(ASCE)0733-9429(2007)133:8(884)

Poggi, D., Katual, G. G., & Albertson, J. D. (2004). A note on the contribution of dispersive fluxes to momentum transfer within canopies. *Boundary-Layer Meteorology*, *111*(3), 615–621. https://doi.org/10.1023/b:boun.0000016563.76874.47

Poggi, D., & Katul, G. G. (2008a). Micro- and macro-dispersive fluxes in canopy flows. *Acta Geophysica*, *56*(3), 778–799. https://doi.org/10.2478/s11600-008-0029-7

Poggi, D., & Katul, G. G. (2008b). The effect of canopy roughness density on the constitutive components of the dispersive stresses. *Experiments in Fluids*, *45*(1), 111–121. https://doi.org/10.1007/s00348-008-0467-7

Poggi, D., Porporato, A., & Ridolfi, L. (2004). The effect of vegetation density on canopy sub-layer turbulence. *Boundary-Layer Meteorology*, *111*(3), 565–587. https://doi.org/10.1023/b:boun.0000016576.05621.73

Raupach, M. R., Finnigan, J. J., & Brunei, Y. (1996). Coherent eddies and turbulence in vegetation canopies: The mixing-layer analogy. *Boundary-Layer Meteorology*, *78*(3–4), 351–382. https://doi.org/10.1007/BF00120941

Righetti, M. (2008). Flow analysis in a channel with flexible vegetation using double-averaging method. *Acta Geophysica*, *56*(3), 801–823. https://doi.org/10.2478/s11600-008-0032-z

Rouse, H. (1937). Modern conceptions of the mechanics of fluid turbulence. *Transactions of the American Society of Civil Engineers*, *102*, 463–505.

Sonnenwald, F., Stovin, V., & Guymer, I. (2019). Estimating drag coefficient for arrays of rigid cylinders representing emergent vegetation. *Journal of Hydraulic Research*, *57*(4), 591–597. https://doi.org/10.1080/00221686.2018.1494050

Spiller, S. M., Rüther, N., & Baumann, B. (2015). Form-induced stress in non-uniform steady and unsteady open channel flow over a static rough bed. *International Journal of Sediment Research*, *30*(4), 297–305. https://doi.org/10.1016/j.ijsrc.2014.10.002

Stoesser, T., & Nikora, V. I. (2008). Flow structure over square bars at intermediate submergence: Large eddy simulation study of bar spacing effect. *Acta Geophysica*, *56*(3), 876–893. https://doi.org/10.2478/s11600-008-0030-1

Tan, G. M., Fang, H. W., Dey, S., & Wu, W. M. (2018). Rui-jin Zhang's research on sediment transport. *Journal of Hydraulic Engineering*, *144*(6), 2518002. https://doi.org/10.1061/(ASCE)HY.1943-7900.0001464

Tanino, Y., & Nepf, H. M. (2008a). Lateral dispersion in random cylinder arrays at high Reynolds number. *Journal of Fluid Mechanics*, *600*, 339–371. https://doi.org/10.1017/S0022112008000505

Tanino, Y., & Nepf, H. M. (2008b). Laboratory investigation of mean drag in a random array of rigid, emergent cylinders. *Journal of Hydraulic Engineering*, *134*(1), 34–41. https://doi.org/10.1061/(ASCE)0733-9429(2008)134:1(34)

Termini, D. (2019). Turbulent mixing and dispersion mechanisms over flexible and dense vegetation. *Acta Geophysica*, *67*(3), 961–970. https://doi.org/10.1007/s11600-019-00272-8

Tsai, C. W., & Huang, S. H. (2019). Modeling suspended sediment transport under influence of turbulence ejection and sweep events. *Water Resources Research*, *55*, 5379–5393. https://doi.org/10.1029/2018WR023493

van Rijn, L. C. (1984). Sediment transport, part II: Suspended load transport. *Journal of Hydraulic Engineering*, *110*(11), 1613–1641. https://doi.org/10.1061/(ASCE)0733-9429(1984)110:11(1613)

Västilä, K., & Järvelä, J. (2018). Characterizing natural riparian vegetation for modeling of flow and suspended sediment transport. *Journal of Soils and Sediments*, *18*(10), 3114–3130. https://doi.org/10.1007/s1136

Wang, W., Huai, W. X., & Gao, M. (2014). Numerical investigation of flow through vegetated multi-stage compound channel. *Journal of Hydrodynamics*, *26*(3), 467–473. https://doi.org/10.1016/S1001-6058(14)60053-6

Wang, X. Y., Xie, W. M., Zhang, D., & He, Q. (2016). Wave and vegetation effects on flow and suspended sediment characteristics: A flume study. *Estuarine, Coastal and Shelf Science*, *182*, 1–11. https://doi.org/10.1016/j.ecss.2016.09.009

Wilson, C. A. M. E. (2007). Flow resistance models for flexible submerged vegetation. *Journal of Hydrology*, *342*(3–4), 213–222. https://doi.org/10.1016/j.jhydrol.2007.04.022

Yang, J. Q., & Nepf, H. M. (2019). Impact of vegetation on bed load transport rate and bedform characteristics. *Water Resources Research*, *55*, 6109–6124. https://doi.org/10.1029/2018WR024404

Yang, W., & Choi, S. (2010). A two-layer approach for depth-limited open-channel flows with submerged vegetation. *Journal of Hydraulic Research*, *48*(4), 466–475. https://doi.org/10.1080/00221686.2010.491649

Yuuki, T., & Okabe, T. (2002). Hydrodynamic mechanism of suspended load on riverbeds vegetated by woody plants. *Proceedings of Hydraulic Engineering*, *46*, 701–706. https://doi.org/10.2208/prohe.46.701

Zhang, R. J., & Xie, J. H. (1989). *River sediment dynamics (in Chinese)*. Beijing, China: China Water and Power Press. ISBN: 9787801244260.